

# Characterization of a microscale cyclical electrical field flow fractionation system

Ameya Kantak, Merugu Srinivas and Bruce Gale\*

Received 28th November 2005, Accepted 2nd March 2006

First published as an Advance Article on the web 14th March 2006

DOI: 10.1039/b516827a

A microscale cyclical electrical field flow fractionation (CyEIFFF) channel is characterized with regard to the effect of various operating parameters and comparison made to recent theoretical developments. Challenges associated with various operating conditions are reported along with some of the optimized operating parameters. The effect of retention wall choice, an offset voltage, relaxation steps, and flow rates, along with the basic operating parameters of voltage, frequency, and electrophoretic mobility are reported. Retention of polystyrene nanoparticle standards is accomplished and the first separations using this technique in a microscale system are also demonstrated. Relaxation steps and offset voltages are found to be effective in eliminating early peaks and in improving plate heights. Plate heights were also found to decrease with increasing flow rates, which is the opposite of the behavior seen in most existing chromatographic systems. The experimental results are compared to the analytical and empirical models of CyEIFFF and found to be compatible. Suggestions are made for improving the separation and analysis methods used with CyEIFFF.

## Introduction

Cyclical electrical field flow fractionation (CyEIFFF) is a recently developed<sup>1,2</sup> member of the field flow fractionation (FFF) family of particle analysis, separation and sample preparation tools first described by Giddings in 1966.<sup>3</sup> FFF methods rely on using an external field perpendicular to a parabolic velocity field within very thin channels. There are several different FFF subtypes based on the choice of an externally applied field, such as: electrical, flow, gravitational, magnetic, sedimentation, steric, thermal and so forth. Significant interest has been shown in electrical FFF systems (EIFFF)<sup>4,5</sup> during the past few years, including the introduction of microscale EIFFF systems.<sup>6</sup> EIFFF systems have been shown to suffer from electrode polarization and an associated effective field decrease to only a fraction of the applied field—typically less than 1%.<sup>4–6</sup> Merugu *et al.*<sup>1</sup> first showed that an alternating electrical field can be applied to reduce the effects of polarization using a macroscale EIFFF system,<sup>2,7</sup> Lao *et al.*<sup>8</sup> demonstrated pulsed EIFFF in a miniaturized system using asymmetric cyclical fields as guided by the work of Mridha *et al.*<sup>9</sup> No CyEIFFF microsystems have been adequately characterized with respect to the theory for cyclical field flow fractionation (CyFFF) originally proposed by Giddings in 1986<sup>10</sup> and extended and demonstrated in sedimentation FFF in 1988.<sup>11</sup> A simulation of cyclical electrical field flow fractionation (CyEIFFF) was published by Stevens in 1990,<sup>12</sup> but not confirmed experimentally. In a recent communication<sup>13</sup> a modified theory of CyFFF for use with electrical systems that was validated using a CyEIFFF microsystem was

reported and work has recently been published related to instrumentation and carrier effects,<sup>14,15</sup> but little information was provided on the operation and characterization of the system.

In this work, a detailed performance evaluation of microscale CyEIFFF will be presented with respect to the operational parameters of the system. A comparison with published analytical models and experimental data will be provided. Basic particle retentions will be shown along with separations and suggestions will be made for improvements in the design and operation of CyEIFFF systems.

## Theory

The theory of CyEIFFF from the literature<sup>10,13</sup> will be used in this work for comparison with experimental data and the reader is referred there for details. Only specifically relevant details are provided here.

A CyEIFFF system is essentially the same as a traditional EIFFF system with two planar electrodes separated by a thin spacer defining a microchannel. The flow in the channel is laminar with Reynolds numbers often less than unity. An oscillating electrical field is provided across the flow channel, such that particles susceptible to the electrical field respond in a manner similar to that shown in Fig. 1. Depending upon the extent of oscillation of the particles in the channel, modes of operation for CyEIFFF are defined.

A dimensionless parameter  $\lambda_o$ , defined for a square waveform by

$$\lambda_o = \frac{\mu E_{\text{eff}}}{2f_w} \quad (1)$$

is used to describe the motion of a particle in a CyEIFFF channel, where,  $\mu$  is the particle electrophoretic mobility,  $f$  is

University of Utah, Department of Mechanical Engineering, 50 S. Central Campus Drive Room 2110, Salt Lake City, UT 84112-9202, USA. E-mail: gale@eng.utah.edu; Fax: (801) 585-9826; Tel: (801) 585-5944

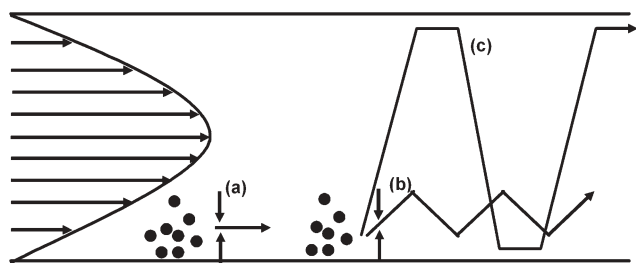


**Fig. 1** Movement of particles in an FFF channel employing (a) EIFFF, (b) CyEIFFF Mode I, and (c) CyEIFFF Mode III.

the frequency,  $E_{\text{eff}}$  is the effective field in the bulk of the channel, and  $w$  is the electrode separation distance. Assuming a particle begins at one wall, if  $\lambda_o < 1$ , the particle cannot reach the opposite wall, and is said to be in Mode I. If  $\lambda_o > 1$ , the particle can reach the opposite wall and is said to be in Mode III. Mode II is where the particle has a grazing incidence at either of the walls with  $\lambda_o = 1$ . Thus, from inspection of eqn (1), the primary user-defined operating conditions in CyEIFFF are the frequency  $f$ , magnitude of the effective electric field  $E_{\text{eff}}$ , and the shape of the applied electric waveform. Effective field is a complex function of the applied voltage, frequency, channel dimensions, electrode materials, and carrier composition, and may be best characterized by measuring electrical parameters of the system.<sup>13</sup> An equivalent circuit of an EIFFF system<sup>16,17</sup> is often used to represent the electrical operation of an EIFFF system with  $C_{\text{DL}}$  and  $R_{\text{DL}}$  in parallel representing the capacitance and resistance of both electrical double layers at the electrode/carrier interface, and in series,  $R_{\text{B}}$ , representing the resistance of the bulk carrier and  $R_{\text{S}}$  representing the resistance of the voltage source. The equation for the effective field in the bulk phase,  $E_{\text{eff}}$  is given by<sup>13</sup>

$$E_{\text{eff}} = \frac{VR_{\text{B}}}{w} \sqrt{\frac{1 + (2\pi f R_{\text{DL}} C_{\text{DL}})^2}{(R_{\text{B}} + R_{\text{S}} + R_{\text{DL}})^2 + (2\pi f (R_{\text{B}} + R_{\text{S}}) R_{\text{DL}} C_{\text{DL}})^2}}, \quad (2)$$

where  $V$  is the applied square wave voltage. In this work, we measured these electrical parameters, and compared the results from the microsystem with the predicted values from the theory given here and previously.<sup>13</sup>

## Experimental

Microscale EIFFF channels of two types were fabricated, gold electrodes on a silicon substrate and bulk graphite channels, using methods described previously<sup>13,17</sup> in order to test the theory for CyEIFFF experimentally and determine best operating practices. Each FFF channel had a length of 5.1 cm, a depth of 30  $\mu\text{m}$ , and width of 5 mm. Graphite microsystems were primarily used for characterization experiments due to their excellent data reproducibility, whereas the results from the gold microsystems lacked repeatability over extended times (typically more than 15–24 hours of continuous operation) due to electrolysis problems and damage to the electrode surfaces. The experimental setup includes: a DC power supply (Agilent, Model E3630A), an AC function generator (Hewlett Packard, Model HP 33120A), a multimeter (Hewlett-Packard, Model HP 34401A), a data acquisition

setup (LabVIEW, National Instruments), and a UV/visible absorbance detector (ESA, Model 520) and is similar to earlier reported system configurations.<sup>13</sup>

The primary carrier used in this work was ultrapure DI water (resistivity 18.2  $\text{M}\Omega \text{ cm}$ ) (EasyPure, Barnstead), however, in some cases, solutions of ammonium carbonate salt in air equilibrated DI water (50 to 100  $\mu\text{M}$ ) was used. The carrier flow was controlled using a syringe pump (KD Scientific) and nanoparticles were injected into the flow channel using Hamilton microliter syringes. The power supplies were used to apply voltage across the CyEIFFF electrodes.

All experiments were performed with polystyrene (PS) and silica particle standards of different sizes (Polysciences, Inc., MA) at a concentration 0.01% by weight and sample volume of 0.2  $\mu\text{L}$  per injection, except for those specifically designed to determine concentration and volume effects. The electrophoretic mobilities of the nanoparticles ranged from  $2.0 \times 10^{-4}$  to  $4.0 \times 10^{-4} \text{ cm}^2 \text{ V}^{-1} \text{ s}^{-1}$ ) as measured using a zeta potential analyzer (Brookhaven Instruments Zeta Plus). The particles were detected at 225 nm on a UV/VIS absorbance detector Model 520 (ESA, Inc, MA) with a flow cell volume of 1.2  $\mu\text{L}$  connected to the end of the microchannel. The output from the detector was acquired using an A/D card attached to a PC and processed using LabVIEW software.

Measured electrical parameter values for the microsystems from time constant and voltage step experiments are listed in Table 1 and were performed as described in ref. 13. To investigate the impact of the source resistance, the voltage drop across the system was measured at various frequencies. A small resistance (10  $\Omega$ ) was added in series with the microsystem, the voltage drop across this resistance was measured, and then the voltage drop across the microsystem was backcalculated.

Since only a little is known about how best to perform CyEIFFF experiments, several experiments were performed varying some basic operating conditions to determine what techniques are best and to allow for maximal understanding when later experiments are performed.

To determine the effect of sample volumes on microscale CyEIFFF experiments, particle standards were injected in the channels using a Hamilton microliter syringe with a resolution of 0.1  $\mu\text{L}$ . Injections of samples at volumes of 0.1  $\mu\text{L}$  to 1.0  $\mu\text{L}$  were performed and plate height measurements made to determine an optimum injection volume. Other preliminary experiments were carried out in order to optimize the performance of the CyEIFFF microsystem. Cyclical square waveforms with a peak-to-peak voltage between zero and 7.0 V (VPP) (*i.e.* up to 3.5 V positive followed by 3.5 V negative) were applied to the microsystem in these experiments. These experiments explored a range of flow rates (0.1–2  $\text{mL h}^{-1}$ ), sample relaxation conditions, choice of accumulation/retention wall, and sample concentration (0.01–0.2  $\mu\text{g mL}^{-1}$ ). Flow rates

**Table 1** CyEIFFF microsystem properties

Carrier type	$R_{\text{B}}/\Omega$	$R_{\text{DL}}/\Omega$	$C_{\text{DL}}/\text{F}$
Ultrapure DI water	880	15100	$198 \times 10^{-9}$
100 $\mu\text{M}$ AC buffer in DI water	595	5790	$748 \times 10^{-9}$
0.5 $\text{mM}$ AC buffer in DI water	76	564	$49 \times 10^{-6}$

above  $2.0 \text{ mL h}^{-1}$  were not used due to the high pressures generated and leakage problems in the fittings. The most practical carrier flow rates were between  $0.5 \text{ mL h}^{-1}$  and  $2.0 \text{ mL h}^{-1}$  for these microsystems; most experiments in this work were carried out at  $1.0 \text{ mL h}^{-1}$  unless otherwise stated.

Stop flow relaxation is a standard method in FFF experiments, however, it has not been used for CyFFF systems. Especially in Mode I where band broadening becomes increasingly an issue, one of the ways to curtail this band broadening could be to use stop flow relaxation to force all particles to a uniform starting location. We tried different combinations of stop flow and offset voltage in order to reduce band broadening during experiments. Sample relaxation was found to be an important step for experiments using the buffered carrier solutions, so in order to achieve relaxation, the carrier flow was completely stopped for about 5 to 7 seconds, and a 0.3 VDC potential was applied to nudge the particles to the accumulation wall in these experiments. This offset voltage was applied during both the stop flow condition and during the normal elution phase of the experiments. Sample recovery experiments were also performed using standard methods.<sup>18</sup>

In the absence of an offset voltage (used to drive particles towards one accumulation wall in Mode I), the particles were observed to elute out much earlier than expected, mostly at the void time. This early peak effect was also shown by Merugu in his work with a macroscale system.<sup>7</sup> A series of experiments with increasing offset voltages were performed to determine the effect of the offset voltage and to search for an optimum value.

Microsystem characterization experiments to understand voltage effects were performed with 100 nm amino-coated polystyrene particles at a constant frequency of 1 Hz, while voltages were varied from 1.0 VPP to 7.0 VPP (square wave). To determine the effect of flow rate, the frequency and voltage were set at 15 Hz and 3.0 VPP, and the flow rates were varied between  $0.5$  and  $2.0 \text{ mL h}^{-1}$ . Experiments over a range of frequencies were performed with a voltage of 3.0 VPP. 100 nm silica ( $2.93 \times 10^{-4} \text{ cm}^2 \text{ V}^{-1} \text{ s}^{-1}$ ) and amino coated polystyrene ( $2.57 \times 10^{-4} \text{ cm}^2 \text{ V}^{-1} \text{ s}^{-1}$ ) particles were used for mobility characterization experiments. Experiments involving a separation of particle fractions were performed with a binary mixture of silica and polystyrene nanoparticles at 3.0 VPP and a  $1.0 \text{ mL h}^{-1}$  flow of ultrapure water (pH  $7.3 \pm 0.1$ ). A comparison between gold and graphite microsystems was performed using both systems at an applied voltage of 4.0 VPP and a range of frequencies.

The experimental run order was randomized to reduce user and instrumental biases. The elution peak values were calculated by taking area moments for every elution profile using Microsoft Excel and Peakfit (SyStat, CA) software. The elution data were reported with a 95% confidence interval and the standard deviation in reported elution times was  $\pm 3$  s. The errors/uncertainties reported in various measurements of elution times were about 7%.

Plate height measurements were made after several experiments to determine the effect of the various parameters on plate height. Plate heights were calculated using standard methods and the plate theory<sup>19</sup> of chromatography, and by assuming that the CyEIFFF microchannel column is linear in nature.

## Results and discussion

### Electrode material effects

In this study it was consistently found that gold microsystems did not provide reproducible results over extended time periods. Visual inspection of the gold electrodes after significant use (requiring disassembly) showed that the electrodes were fouling or disintegrating over time. Electrical currents were not reproducible in the gold electrode microsystems, and short circuiting occurred after extended time periods of use (more than 24 hours). On the other hand, graphite electrode microsystems were consistent, reproducible, and for reasons unknown at this time, showed better retention of nanoparticles.

Graphite electrodes were found to be better electrodes than their gold counterparts for a number of reasons, not least of which was the fact that graphite electrodes were much more robust. Graphite was also found to be better for retention as shown in Fig. 2. Clearly, the retentions in the graphite system were better than those in the gold microsystem. In addition, the extent of band broadening was higher in the gold microsystem, and the peaks were almost flat at higher frequencies (above 10 Hz). Additionally, gold microsystems were not repeatable over extended periods of time. Thus, the graphite systems not only produced consistent results, they produced better results. The primary reason appears to be that the effective fields in the gold systems are much lower than in the graphite systems. The low effective fields appear to be associated with high losses at the electrode/carrier interface in the gold systems.

### Sample volume and concentration effects

To determine the effect of sample volumes on microscale CyEIFFF experiments, a series of particle retention experiments with increasing sample volumes were performed. Injections with  $0.1 \mu\text{L}$  sample volume were problematic in

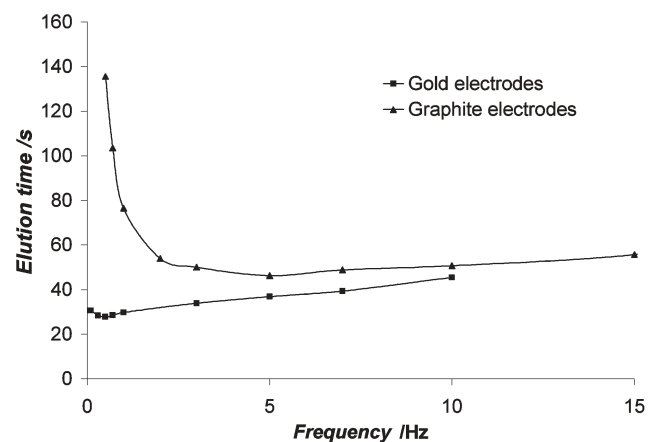


**Fig. 2** A comparative study of performance of gold and graphite microsystems with 100 nm polystyrene nanoparticles. Note that retentions in the gold microsystem are consistently lower than those in the graphite microsystems. The extent of band broadening was also greater in the gold microsystem. The results were obtained at carrier flow of DI water  $1.0 \text{ mL h}^{-1}$ , applied voltage was 4.0 VPP square wave with no offset voltage used in Mode I experiments.

that many times injections were found to be noisy with no significant levels of absorbance detection. Further, the 0.1  $\mu\text{L}$  sample did not result in any significant reduction in plate heights. Therefore, the experiments were conducted with 0.2  $\mu\text{L}$  consistently. Larger volumes increased plate heights without providing significantly better signal-to-noise ratios.

Particle concentrations were varied to determine their effect on plate heights (see Fig. 3) and it was observed that plate heights dropped along with sample particle concentration. In order to have consistent and observable particle peaks, the sample concentration for the characterization experiments was kept at 0.01% by weight. The absolute sample recovery experiments showed that about 87 to 94% of the injected samples were recovered in most experiments.

### Retention wall choice

In Mode III experiments, where particles travel from wall-to-wall, a choice of accumulation wall is unnecessary and meaningless. However, in Mode I, where the particles predominantly oscillate near one of the walls, the choice of the accumulation wall may be important. The wall containing entrance and exit ports was chosen to be the accumulation wall due to the obvious advantage offered in reducing band broadening effects as shown in Fig. 4. The reason for why the wall containing the ports should be the accumulation wall seems readily apparent, in that particles that reach the end of the channel can quickly be delivered to the detector, while particles at the opposite wall will only be drawn slowly into the exit port, and thus spread over time and volume, as seen in Fig. 4.

### Offset voltage

The magnitude of the offset voltage during relaxation and during the experimental run can help eliminate early peaks, but can also modify the retention results. An offset voltage applied throughout the experiment was found to increase the particle elution times as the magnitude of the offset increased, as

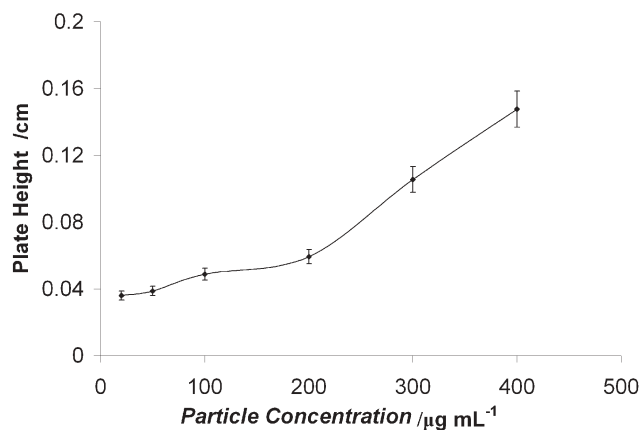


**Fig. 3** Plate height data for particle concentrations in  $\mu\text{g mL}^{-1}$  (averaged). The results were obtained for 100 nm amino end group polystyrene (PS) particles in ultrapure DI water carrier (18.2  $\text{M}\Omega\text{ cm}$ ) flowing at  $2.0\text{ mL h}^{-1}$  in the graphite microsystem. The applied field was at 3.0 VPP square wave with a frequency of 10 Hz.

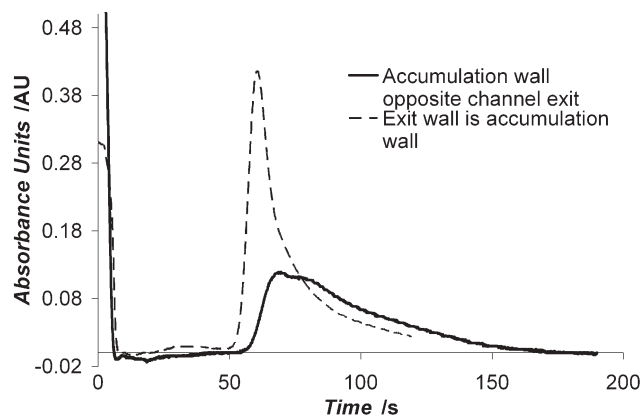


**Fig. 4** 100 nm amino end PS particles in Mode I under two different accumulation wall conditions; the applied voltage was 3 VPP squarewave with frequency 7 Hz; 50  $\mu\text{M}$  ammonium carbonate solution was the carrier at  $1.0\text{ mL h}^{-1}$  with a stop flow relaxation of 5 s. The results were obtained in the graphite microsystem.

shown in Fig. 5. The reason for this increase seems clear in that particles under the influence of the offset voltage will spend more time than they otherwise might near the wall, and will therefore travel more slowly through the separation channel. At high offset voltages, the technique may become more like normal EIFFF than CyEIFFF. Even the small 0.3 V DC offset is sufficient to reduce the early peaks significantly. Hence, it is recommended that offset voltages above 0.3 VDC should not be used to enable proper interpretation of the results. Applying an offset voltage does not significantly affect the predicted elution time from CyEIFFF theory and the observed elution times remain within the statistical error of  $\pm 3\text{ s}$ . No observable changes within statistically significant limits in

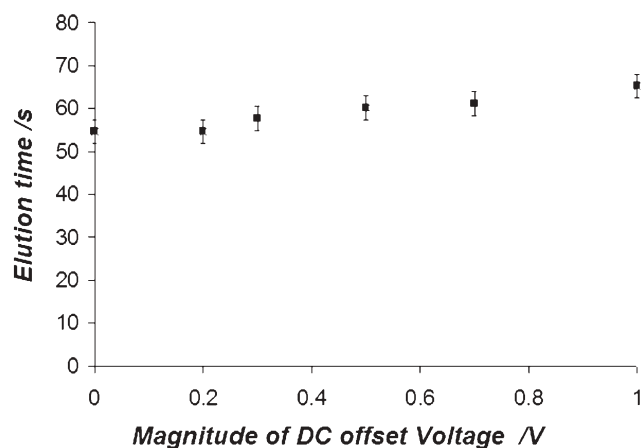


**Fig. 5** Performance of a graphite microsystem with a series of increasing DC offset voltages applied. The data shown here is for an applied voltage of 3.0 VPP, a frequency of 7 Hz, and an air-equilibrated, 50  $\mu\text{M}$  ammonium carbonate carrier. Zero and 0.2 V showed similar responses. As the offset magnitude was increased, elution time also increased. The time deviation between the 0 V case and that for 0.3 V case was within acceptable statistical limits (3.0 s); the higher offset voltages showed increasing deviations implying that the offset voltage affects the performance, and should be used cautiously.

elution times were obtained for 0.1 and 0.2 VDC offset voltages.

### Stop flow relaxation

Several different combinations of relaxation or stop flow and offset voltages were tried to determine if one operating combination was superior. From Fig. 6 it is apparent that simultaneously applying stop flow and an offset DC voltage at sample injection is better than the other methods, and is recommended for reducing band broadening effects. The sustained offset voltage was therefore used for all of the following experiments shown in this work. With an offset voltage only, and no stop flow, band broadening was shown to increase; hence, we recommend stop flow relaxation, especially when the experimental conditions generate very small values of  $\lambda_0$ .

### Applied voltage effects

Previous work on CyEIFFF<sup>13</sup> has found that the source resistance is an important component of the entire electrical system and the voltage drop across it becomes increasingly important as the frequency of the applied field increases. The applied voltage begins to drop across the source resistance when the microsystem resistance becomes comparable with the source resistance value. This large drop in resistance occurs in two situations: high carrier ionic concentrations or higher frequencies with the actual frequency where this change occurs dependent on the materials, geometry, and carrier used. Failure to consider the source resistance in cases where the impedance across the EIFFF system becomes small can lead to erroneous conclusions.

Accordingly, the voltage drops for two carriers in a graphite microsystem are summarized in Table 2. The voltage measured across the microsystem was shown to decrease in magnitude when the frequency of the applied voltage was increased. This

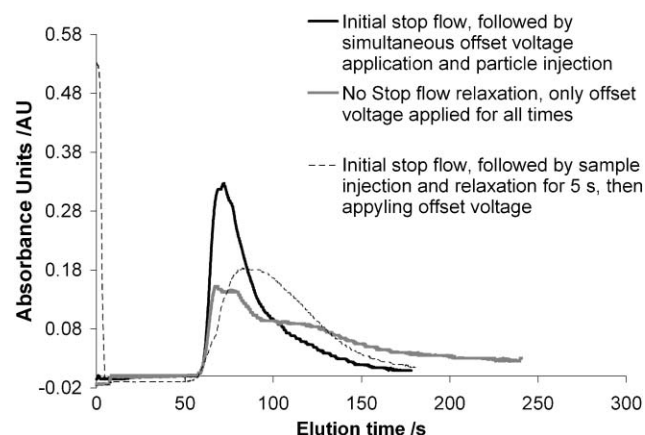


**Fig. 6** Sample relaxation schemes: An offset applied all the time distorts the shape of the peak, whereas, the relaxation procedures reduce broadening of the peak. The applied voltage was 3.0 VPP with 0.3 VDC offset voltage. The frequency was 7 Hz and carrier was air equilibrated DI water with a flow rate of 1.0 mL h<sup>-1</sup> for these experiments with 100 nm polystyrene particles. The graphite system was used in these experiments.

decrease would suggest that the voltage across the bulk carrier (where retention is generated) decreases with increasing frequency, which could limit the value of using cyclical fields, but the reason for the drop in voltage across the channel is that the relative magnitude of the resistance across the channel was falling when compared to other resistances in the circuit. The measured values of  $R_{DL}$ ,  $C_{DL}$ , and  $R_B$  were 6950  $\Omega$ , 453 nF and 558  $\Omega$  with a source resistance of 60  $\Omega$  for an air equilibrated DI water carrier. At a frequency of 1 Hz, the voltage drop caused by the impedance of the electrical double layers (6930  $\Omega$  at a frequency of 1 Hz) was 1.84 V with a voltage drop across  $R_B$  of 0.147 V and across the source resistance of 0.016 V. When the frequency was increased to 300 Hz, the impedance of the electrical double layers went down from 6930  $\Omega$  to 1400  $\Omega$ . Due to this change in impedance, the voltage drop across the impedance of the electrical double layers is now 1.39 V, and that across  $R_B$  and is  $R_S$  now 0.531 V and 0.08 V respectively. These calculations based on the circuit model show that when the frequency is small, e.g., 1 Hz, the overall voltage drop across the microsystem (1.84 V + 0.147 V = 1.99 V) was near the applied voltage of 2.00 V and close to the measured value of 1.99 V at 1 Hz. When the frequency was increased to 300 Hz, the overall voltage drop across the microsystem was (1.39 V + 0.531 V =) 1.92 V with an increased drop across the source resistance of 0.08 V. This simple calculation shows that with an increase in frequency, and the associated drop in impedance of the electrical double layers, there is a definite increase in the voltage drop across the bulk carrier, while there was a decrease in overall voltage across the microsystem alone! Thus, a measure of the voltage drop across the FFF channel is not sufficient for predicting the effective electric field in an EIFFF channel, and a researcher must be careful in determining what voltage is actually applied across the carrier solution, since the value may be different from that shown on a power supply. After evaluation of electrical parameters, one should be able to calculate the theoretical voltage distribution to arrive at appropriate values of the effective field, which in this event happens to be 7.39% at 1 Hz and 26% at 300 Hz of the applied nominal field value. In summary, with increasing frequency, the impedance of the microsystem decreases, while the effective field in the microchannel increases. These effects are consistent with previous studies by Palkar *et al.*<sup>16,20</sup> in EIFFF systems.

**Table 2** Measured voltages across the microsystem showing the effect of frequency and source resistance on voltage distribution. The source resistance was 50  $\Omega$  with additional 10  $\Omega$  resistance in series, the applied voltage was a 2.0 VPP squarewave, and the carrier flow rate was 1.0 mL h<sup>-1</sup>

Frequency/ Hz	DI water pH 7.3		50 $\mu$ M ammonium carbonate solution in DI water (pH 8.2)	
	Measured VPP	Fraction of applied voltage	Measured VPP	Fraction of applied voltage
1	1.99	0.99	1.98	0.99
5	1.98	0.99	1.92	0.96
10	1.93	0.97	1.86	0.93
50	1.92	0.96	1.67	0.83
100	1.91	0.95	1.56	0.78
200	1.90	0.95	1.45	0.72

After determining the electrical field in the channel and optimizing the retention conditions for the current setup of the system, characterization experiments were performed.

### Characterization experiments

Particle retention in CyEIFFF is anticipated to be a function of applied voltage, frequency, electrophoretic mobility, flow rate, ionic strength and channel geometry. Except for the last two, each of these parameters were varied independently in these experiments with careful attention provided to mode transition to prevent improper data interpretation.

### Frequency effects

Basic retention experiments with polystyrene particles were performed for a range of frequencies and different voltages. The elution times for a series of experiments with 100 nm amino end group polystyrene particles in the graphite microsystem are shown in Fig. 7. The mode transition was observed at 5 Hz, 7 Hz and 10 Hz for the applied voltage values of 3.0 VPP, 4.0 VPP and 5.0 VPP respectively and these frequencies correspond to measured  $\lambda_o$  values of unity. How these measured values of  $\lambda_o$  compare to theory will be discussed later.

In Mode III for any given applied voltage, as the frequency of the applied voltage was increased (up to the mode transition frequency), the elution time of the particles decreased as is consistent with the theory of CyEIFFF.<sup>2,13</sup> In Mode I, as the frequency of the applied voltage was increased, the particles again began eluting later. As the frequency of the applied field was increased in Mode I, the particle elution time increased with frequency. Similar behavior was observed for these particles at all three applied voltages. This behavior agrees with the theoretical predicted particle behavior in Mode I.<sup>2,13</sup> One can also observe that due to an increase in applied voltage, the elution curves in Fig. 7 move to the right. This behavior is also consistent with the theory.

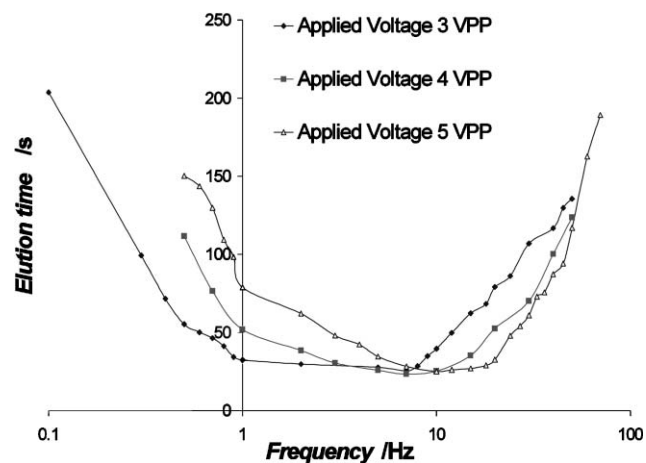


**Fig. 7** Effect of frequency variation on retention times: Elution curves for 100 nm polystyrene nanoparticles at three different applied squarewave voltages. The carrier used was ultrapure DI water at pH 7.1 and 1.0 mL h<sup>-1</sup> in a graphite electrode microsystem.

### Voltage effects

A summary elution curve for varying voltages is shown in Fig. 8. At 7.0 VPP the electrolysis of water and bubble generation was vigorous. At 6.5 VPP, electrolysis was more sporadic, but the data had a very low signal-to-noise ratio, so the results for both voltages are not reported. As the voltage was increased from 2.0 VPP to 6.0 VPP, there was an increase in the elution time. Similarly when the voltage was decreased from 1.5 VPP to 1.0 VPP, there was an increase in the elution time. The first phenomenon indicates that the particles were in Mode III, while the second indicates that they were in Mode I. Again this behavior is consistent with the theory, which will be explored in more depth later. The effect of varying electrophoretic mobility is similar to that of voltage variation and is discussed in the next section.

### Electrophoretic mobility and particle size effects

The separation mechanism in CyEIFFF is based primarily on differential electrophoretic mobilities.<sup>2,13</sup> Ideally, two particles with the same diameter but different electrophoretic mobilities should have different elution times. Two particles with the same electrophoretic mobilities, but different diameters should have the same elution time as well. However, elution times may not be the same primarily due to diffusion or steric effects. These effects are known to be small, but not inconsequential.<sup>13</sup>

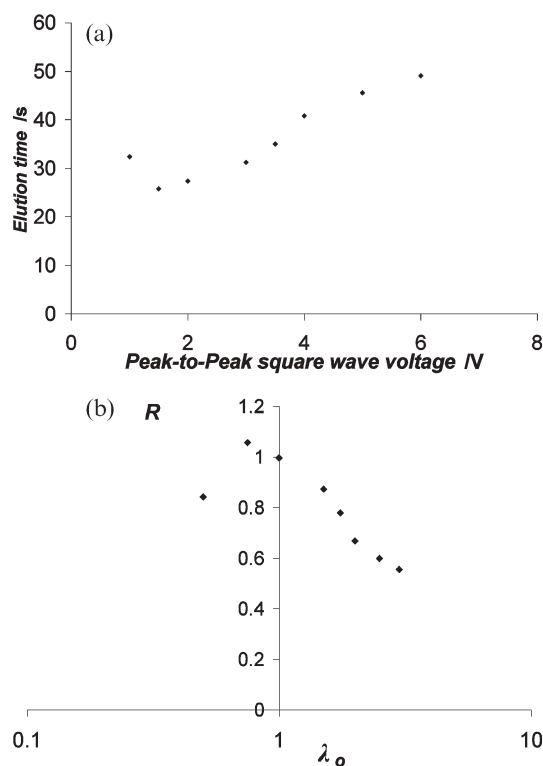


**Fig. 8** Effect of varying applied voltage in a CyEIFFF graphite system with 100 nm amino coated polystyrene particles; the carrier was a 50  $\mu$ M ammonium carbonate solution flowing at 1.0 mL hr<sup>-1</sup>. The applied frequency was 1 Hz. Part (a) shows changes in elution times with voltage change whereas, part (b) shows the same data as dimensionless retention parameter  $\lambda_o$  and retention ratio  $R$ .

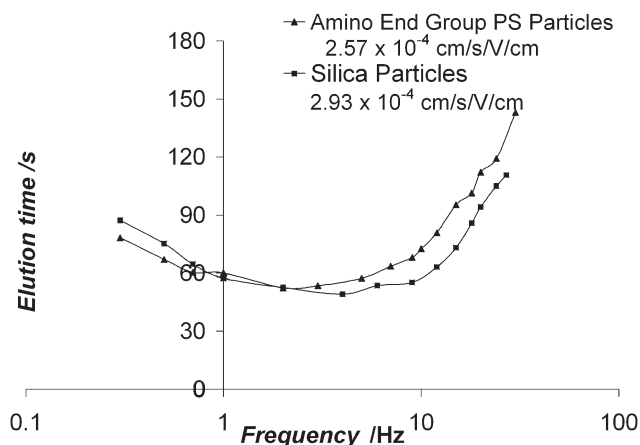


**Fig. 9** Two populations of 100 nm particles (with different electrophoretic mobilities) elution times at 1.0 mL h<sup>-1</sup> (no stop flow relaxation) and 3.0 VPP with no offset. The carrier was ultrapure DI water with resistivity 18.2 MΩ cm in a graphite microsystem.

Elution times are shown in Fig. 9 for 100 nm silica and amino coated polystyrene nanoparticles with different electrophoretic mobility values. The elution times show that the curve for the higher mobility has shifted to the right, which agrees with the theory for CyEIFFF.

Additional experiments were conducted using nanoparticles with different sizes but similar electrophoretic mobility values as shown in Fig. 10. The diameters of the amino coated polystyrene particles were 100 nm and 202 nm with nearly identical measured mobility values ( $2.57 \times 10^{-4}$  and  $2.54 \times 10^{-4}$  cm<sup>2</sup> V<sup>-1</sup> s<sup>-1</sup> respectively). The experiments yielded statistically inseparable elution times in most cases (elution time difference being less than 5 s) suggesting no significant dependence on particle size for the tested particle size range.

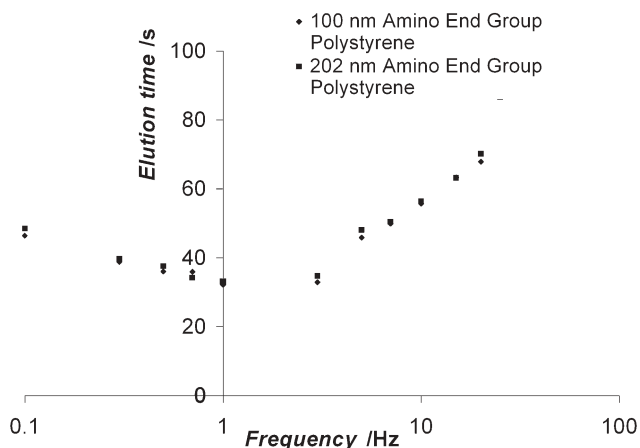


**Fig. 10** Elution times for 100 nm amino end group and 202 nm polystyrene nanoparticles with nearly identical measured electrophoretic mobility values ( $2.57 \times 10^{-4}$  cm<sup>2</sup> V<sup>-1</sup> s<sup>-1</sup>). No significant size effect was present. The carrier flow is 1.0 mL h<sup>-1</sup> (with stop flow at injection) in a graphite microsystem. The applied voltage is 3.0 VPP with a 0.3 VDC offset and stop flow relaxation.

## Flow rate effects

In previous work by Gale<sup>21</sup> in EIFFF microsystems, and by Merugu<sup>1,2</sup> in CyEIFFF macrosystems, it was shown that the effect of flow rates on the retention ratio was not significant. In the theory of CyEIFFF the retention ratio does not depend on the carrier flow rate, and elution time decreases linearly with an increase in flow rate. Flow rate should not affect the mode of operation in CyEIFFF. While the data are not given here, flow rate change was shown to have little impact on retention ratio.

However, an interesting effect was discovered when the flow rate was changed. The plate heights actually decreased with increasing flow rates as shown in Fig. 11, which is the opposite of the trend seen in most chromatographic systems. The reason behind this effect is associated with the mechanism of CyEIFFF. The particle residence time in the channel increases as the flow rate decreases. Due to this increased residence time, diffusion tends to disperse the particle cloud more, and band broadening increases. In normal FFF systems, non-equilibrium effects are significant, and slower flow rates allow the system to move closer to equilibrium, giving better plate heights. CyFFF is not based on equilibrium, so plate heights increase the longer that dispersive effects are allowed to act. This phenomenon could be an added advantage to CyFFF systems, since it might allow faster, better resolved separations.

## Plate heights

Band broadening is an undesirable event in separation technologies since it decreases the resolution of the separation system. From the particle retention experiments it was clear that band broadening in CyEIFFF microsystem occurred as particles moved into the extremes of either Mode I or III. A plot of plate heights for 100 nm amino end group polystyrene particles for elution profiles at 3.0 VPP applied square wave voltage in ultrapure DI water carrier is shown in Fig. 12. A smaller value of plate height indicates a better separation system, and also gives a quantitative measurement of the extent of band broadening. From these plots it is evident that

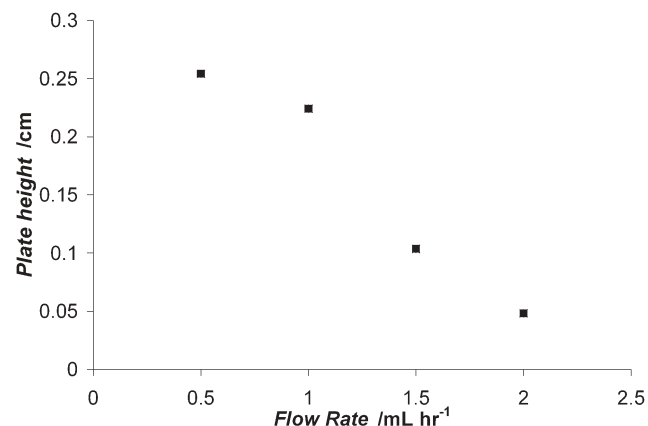


**Fig. 11** Performance of the graphite microsystem in Mode I at 3.0 VPP and 15 Hz with ultrapure DI water carrier (pH 7.05) and 0.3 VDC applied offset voltage with flow relaxation. The flow rate was varied and the plate heights are measured. Band broadening increases as the flow rate was decreased.

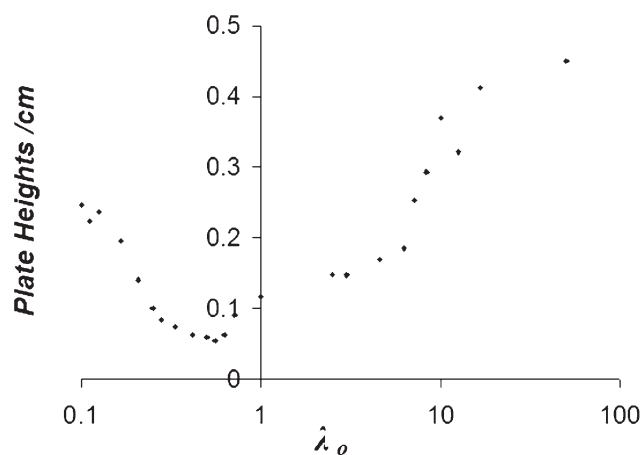


**Fig. 12** Band broadening in the graphite microsystem: plate height calculations for 100 nm amino end group particles at 3.0 VPP square wave in ultrapure DI water carrier at  $1.0 \text{ mL h}^{-1}$ ; broadening was the lowest near the mode transition frequency with the least plate height. No flow relaxation or offset voltage was used in these experiments.

band broadening is low near the transition of modes. Near the mode transition region, which corresponds to either side of the transition frequencies (about 5–7 Hz) the plate heights increased suggesting that the band broadening effects had increased. A similar trend was observed in macroscale CyEIFFF system in earlier works by Merugu.<sup>2</sup>

The level of band broadening was consistent for all applied voltages and it was the major factor limiting the operating range of the microsystem. Extremely wide peaks as well as very low signal-to-noise ratios were obtained for very high frequencies (above 75 Hz), limiting the operation of CyEIFFF system at this time. We propose as an explanation that the coherence of the particle cloud becomes weaker as time passes with the particles in the channel. Dispersion effects (particle diffusion, wall interactions *etc.*) are allowed to collect over time and increase band broadening. As was shown in Fig. 11, band broadening falls with an increase in flow rate and a reduction in the residence time in the channel. Thus, the best way to reduce plate heights in CyFFF systems may be by increasing the flow rate significantly, especially when experiments generating high retention are performed (conditions far from  $\lambda_o = 1$ ). In our view band broadening remains a major factor limiting the performance of CyEIFFF systems, and reducing plate heights under high retention conditions should be the most important task for workers in this field.

#### Separations in CyEIFFF: Application and current limitations

The goal of a CyEIFFF system is not only to retain and characterize particles, but also to separate particles in a mixture. CyEIFFF separations are based on differences in electrophoretic mobilities. The application of CyEIFFF to separating a binary particle mixture (100 nm silica particles and amino end group 100 nm polystyrene particles) is shown in Fig. 13. At low frequencies (below 7 Hz) there is virtually no separation of particles which is evident from a single peak. From individual particle runs, it was clear that the electrophoretic mobility of the silica particles was higher than that of

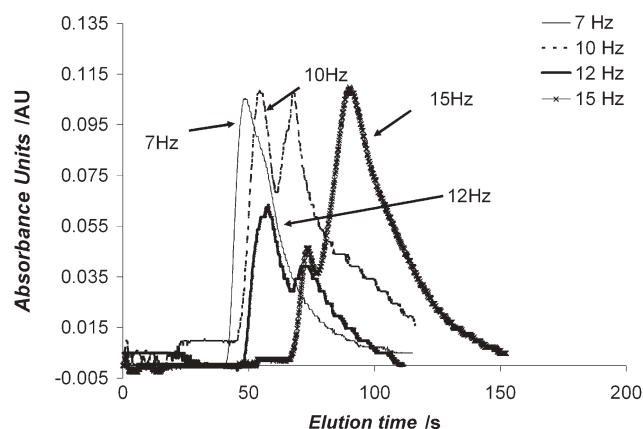


**Fig. 13** Simultaneous fractionation of 100 nm silica nanoparticles and polystyrene (PS) amino end group nanoparticles. The applied voltage was 3.0 VPP with a 0.3 VDC offset and stop flow relaxation. A DI water carrier at  $\text{pH } 7.4 \pm 0.1$  and  $1.0 \text{ mL h}^{-1}$  flow rate is used. The first peak is of silica nanoparticles and the latter one PS nanoparticles. The individual particle fractions were confirmed using individual particle run fractograms under identical experimental conditions.

the polystyrene particles, suggesting that in Mode I, the polystyrene particles would elute out later than the silica particles. As the frequency of the applied voltage was increased to 12 Hz, separation became evident from the two particle peaks in the same elution fractogram, although the peaks were not well resolved. As the frequency was increased further to 15 Hz, the separation became more evident. A further increase in frequency led to band broadening with no apparent gain in peak resolution, and hence, those results are not shown here. The individual particle elution times were compared with those in the mixture, and they matched with individual particle elution times within acceptable statistical limits. The separations with  $100 \mu\text{M}$  salt solution of ammonium carbonate in DI water were also achieved but not shown here. However, with a DI water carrier, the resolution was clearly better than that observed for the  $100 \mu\text{M}$  salt solution. Also, the signal noise and band broadening were smaller with a DI water carrier than with the salt solution carrier.

To improve separations in microscale CyEIFFF systems, contributions to dispersion need to be minimized. The primary source of band broadening in current microscale CyEIFFF systems is the off-chip detector. Although the tubing connecting the channel and detector was kept as short as possible, it still contributed to band broadening. The detection of the particles occurred after a dead time of 13 s, which is a substantial period for the mixing of the two particle fractions. Further, the flow cell volume was comparatively large ( $1.2 \mu\text{L}$  which was 15.7% of the total channel volume of the microsystem) which also contributed to the mixing of the two fractions. Using the same flow cell for a macroscale system<sup>7</sup> makes the flow cell volume only 0.53% of the channel volume, which gave well-defined, better resolved peaks.<sup>2</sup> Given these experimental limitations, it was still interesting to see that there was an observable separation with measurable resolution between the two particle fractions. Separation or resolution would benefit if the flow cell volume can be made very small, and the detection is made on-chip.

A final observation regarding the time required for particle separation in the CyEIFFF microsystem may be helpful. The separations in Fig. 13 were achieved in less than three minutes, indicating a possible strength of the system in achieving fast separations. Separations were also observed at small voltages of 3.0 VPP, which is three orders of magnitude less than the conventional electrophoretic separation systems. With better detection (possibly on-chip) and fraction collection schemes, faster and better resolved separations may be achieved.

### Comparison with the theory

The results from the particle retention experiments were compared with the CyEIFFF theory using the lumped electrical parameter model to calculate the effective fields in the channel.<sup>13</sup> Using the electrical parameter values from Table 1, the results were shown to agree well with the theoretical trends as shown in Fig. 14. Mode transition was predicted reasonably well using the model and similar trends were experimentally shown in the microsystem. Thus, it may be concluded that the mechanism of CyEIFFF in a microsystem can be represented well with the lumped electrical parameter model. Based on this model, the effective field within the microsystem was estimated to be 12 to 13% in the case of ultrapure DI water and about 6 to 7% with air equilibrated DI water. It was evident that the system dynamics were governed mostly by electrical effects more than by any other effect mentioned in the model. Note that the effective fields found in the microscale systems were much smaller than those generated in the macroscale systems. The scaling of these systems is such that the higher capacitances are better for generating high fields in AC conditions. Thus larger systems will generate higher fields, but there should be a channel size that optimizes both electrical properties and the benefits of smaller channels. The precise dimensions of such a channel are not known at this time, and may vary with the electrode material used in the system.

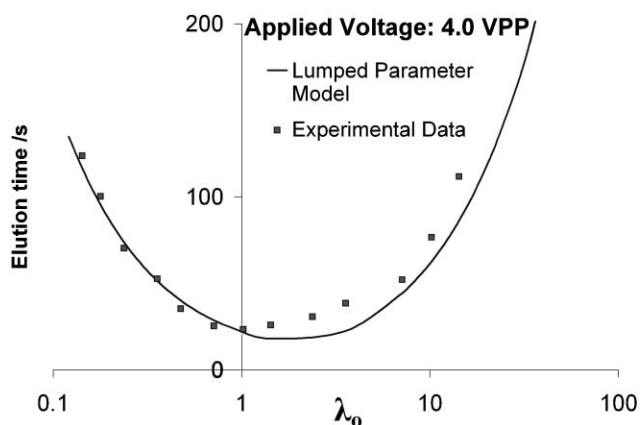


**Fig. 14** Comparison between the results predicted using the lumped parameter model<sup>13</sup> and the experimental data at 3.0 VPP. The particle electrophoretic mobility was  $2.57 \times 10^{-4} \text{ cm}^2 \text{ V}^{-1} \text{ s}^{-1}$ . The flow rate of the carrier (ultrapure DI water with resistivity  $18.2 \text{ M}\Omega \text{ cm}$ ) was  $1.0 \text{ mL h}^{-1}$ , and no stop flow or offset voltage was used. Properties for the bulk voltage estimation used were as detailed in the caption to Table 2.

### Conclusion

An understanding of the effect of various operating parameters in microscale CyEIFFF was achieved in this work, which clearly depict its operational range and limitations for the first time. Some of the experimental optimization techniques developed in this work such as choice of accumulation wall, direction and magnitude of offset voltage, and stop flow relaxation will be useful for future researchers in optimizing or facilitating experimental analysis. The system performance was thoroughly evaluated at various frequencies, voltages, electrophoretic mobilities, flow rates, and for a few particle sizes and it was shown that the trends in the microscale CyEIFFF system are similar to those in the macroscale system and those predicted by theory. The first successful separations in a microscale system were achieved in this work from the binary sample mixtures of nanoparticle standards at low applied fields with speed, but their separation resolution was not good due to band broadening and dispersion effects. Such broadening was observed at very low and very high frequencies and was the most important performance limiting factor of CyEIFFF in general, but may possibly be resolved by increasing the flow rates used in the experiments. The band broadening effect was also quantified in this work using the chromatographic plate theory. It was also shown in this work that the graphite electrode microsystems were more robust and reliable in performance than gold electrode microsystems.

There are important areas which have not been explored in this work, which should be carefully examined. The first of these includes the performance of CyEIFFF at different ionic strengths. This characterization of the CyEIFFF system will be extremely important from the point of view of biological sample preparation, which normally requires buffer solutions of high ionic strengths. It appears likely, based on previous work by Palkar and coworkers,<sup>16,20</sup> that retentions in CyEIFFF systems would decrease with increasing ionic strength. Additionally, issues like band broadening and dispersion in CyEIFFF need to be addressed by using better detection schemes (probably on-chip) and smaller, more sensitive detectors. Since this separation method is based on differential electrophoretic mobilities, it has the potential to have a significant impact on separation science. Expected applications include separating nanoparticles or biomolecules based on their differential mobilities, evaluating their surface charge, and preparing biological samples for laboratory assays. Nucleic acids, proteins, liposomes, viruses, and cells may all be amenable to characterization and processing using CyEIFFF.

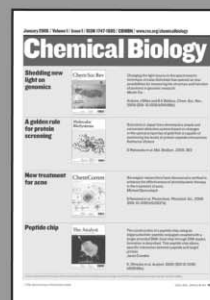
### References

- 1 S. Merugu, *Master's Thesis*, Louisiana Tech University, LA, 2003.
- 2 B. K. Gale and S. Merugu, *Electrophoresis*, 2005, **26**, 9, 1623–1632.
- 3 J. C. Giddings, in *Field-flow fractionation handbook*, ed. M. Schimpf, K. Caldwell, and J. C. Giddings, John Wiley & Sons, Inc., New York, 2000, ch. 1.
- 4 M. Dunkel, N. Tri, R. Beckett and K. Caldwell, *J. Microcolumn Sep.*, 1997, **9**, 177–183.
- 5 M. Schimpf and K. Caldwell, *Am. Lab.*, 1995, **27**, 64–68.
- 6 B. K. Gale, K. D. Caldwell and A. B. Frazier, *IEEE Trans. Biomed. Eng.*, 1998, **45**, 12, 1459–1469.

- 7 M. Srinivas and K. Gale, Cyclical Electrical Field Flow Fractionation, in *Proceedings of the 10th International Symposium on Field Flow Fractionation, Amsterdam, Netherlands, July 2–5, 2002*, p. P32.
- 8 A. I. K. Lao, D. Trau and I. M. Hsing, *Anal. Chem.*, 2002, **74**, 5364–5369.
- 9 C. H. Mridha, S. Siew, Y. K. Sarkar and G. Chan, *Mater. Res. Soc. Symp. Proc.*, 2000, **612**, D911–D917.
- 10 J. C. Giddings, *Anal. Chem.*, 1986, **58**, 2052–2056.
- 11 S. Lee, M. N. Myers, R. Beckett and J. C. Giddings, *Anal. Chem.*, 1988, **60**, 1129–1135.
- 12 F. J. Stevens, *J. Biochem. Biophys. Methods*, 1990, **20**, 275–292.
- 13 A. S. Kantak, S. Merugu and B. K. Gale, *Electrophoresis*, in press.
- 14 T. Masudo and T. Okada, *J. Chromatogr., A*, 2006, **1106**, 196–204.
- 15 A. S. Kantak, S. Merugu and B. K. Gale, *Anal. Chem.*, 2006, DOI: 10.1021/ac052127i.
- 16 S. A. Palkar and M. R. Schure, *Anal. Chem.*, 1997, **69**, 16, 3223–3229.
- 17 B. K. Gale, K. D. Caldwell and A. B. Frazier, *Anal. Chem.*, 2002, **74**, 1024–1030.
- 18 S. K. Ratanathanawongs-Williams and J. C. Giddings, *Field flow fractionation handbook*, ed. M. Schimpf, K. Caldwell and J. C. Giddings, John Wiley and Sons Inc., NY, 2000, ch. 21.
- 19 M. R. Ladisch, *Bioseparations engineering: Principles, practice and economics*, John Wiley & Sons, New York, 2001, ch. 1.
- 20 S. A. Palkar and M. R. Schure, *Anal. Chem.*, 1997, **69**, 16, 3230–3238.
- 21 B. K. Gale, K. D. Caldwell and A. B. Frazier, *Anal. Chem.*, 2001, **73**, 10, 2345–2352.

# Chemical Biology

An exciting news supplement providing a snapshot of the latest developments in chemical biology



Free online and in print issues of selected RSC journals!\*

**Research Highlights** – newsworthy articles and significant scientific advances

**Essential Elements** – latest developments from RSC publications

**Free links** to the full research paper from every online article during month of publication

\*A separately issued print subscription is also available

RSC Publishing

[www.rsc.org/chemicalbiology](http://www.rsc.org/chemicalbiology)

30110553